

# Integrated Dynamic Simulation of Rapid Thermal Chemical Vapor Deposition of Polysilicon

Guangquan Lu, Monalisa Bora, Laura L. Tedder, and Gary W. Rubloff, *Senior Member, IEEE*

**Abstract**—A physically-based dynamic simulator has been constructed to investigate the time-dependent behavior of equipment, process, sensor, and control systems for rapid thermal chemical vapor deposition (RTCVD) of polysilicon from  $\text{SiH}_4$ . The simulator captures the essential physics and chemistry of mass transport, heat transfer, and chemical kinetics of the RTCVD process as embodied in equipment. In order to complete the system-level description, reduced-order models are also employed to represent processes involving high complexity of physics. Integration of individual simulator elements for equipment, process, sensors, and control systems enables the evaluation of not only the deposition rate and film thickness, but also of a broad range of dynamic system properties such as equipment performance, gas flow conditions, wafer temperature variation, wafer optical properties (absorptivity/emissivity), reaction gas composition, total process cycle time, consumables volume, and reactant utilization. This makes the simulator directly applicable to the optimization of process recipes and equipment design, to process control strategy, and to fault classification. This case study of polysilicon RTCVD demonstrates 1) that integrated dynamic simulation is a versatile tool for representing system-level dynamics and 2) that such representation is pivotal in successful applications of modeling and simulation for manufacturing optimization and control.

**Index Terms**—CVD, semiconductor process modeling, simulation.

## I. INTRODUCTION

COMPUTER simulation has played a pivotal role in some crucial aspects of the semiconductor manufacturing industry. Recently, interest has been growing to exploit simulation for understanding process dynamics and for process control applications [1]–[3]. The simulation research

Manuscript received April 22, 1996; revised July 7, 1997. This work was supported by the Semiconductor Research Corporation, Grant SRC 95-BP-132, and by the National Science Foundation, Grants CDR 8721505 and EEC-9526147.

G. Lu was with the NSF Engineering Research Center for Advanced Electronic Materials Processing, North Carolina State University, Raleigh, NC 27695 USA. He is now with Novellus Systems Inc., San Jose, CA 95134 USA (e-mail: brian.lu@novellus.com).

M. Bora was with the NSF Engineering Research Center for Advanced Electronic Materials Processing, North Carolina State University, Raleigh, NC 27695 USA. She is now with is with the Actel Corporation, Sunnyvale, CA 94086-4533 USA (e-mail: bora@actel.com).

L. L. Tedder was with the NSF Engineering Research Center for Advanced Electronic Materials Processing, North Carolina State University, Raleigh, NC 27695 USA. She is now with the Optoelectronic Computing Systems Center, University of Colorado, Boulder, CO 80309-0525 USA (e-mail: tedderl@colorado.edu).

G. W. Rubloff was with the NSF Engineering Research Center for Advanced Electronic Materials Processing, North Carolina State University, Raleigh, NC 27695 USA. He is now with the Institute of Systems Research and Department of Materials and Nuclear Engineering, University of Maryland, College Park, MD 20742-3285 USA (e-mail: rubloff@isr.umd.edu).

Publisher Item Identifier S 0894-6507(98)00334-0.

effort in this paper is focused on coherently investigating the *system-level dynamic* behavior of process, equipment, sensors, and controls of a rapid thermal chemical vapor deposition (RTCVD) system. Polysilicon RTCVD is used as an example to illustrate the potential of this simulation technique in design, optimization [2], and control of processes and equipment for the development of environmentally-conscious manufacturing technologies.

The mathematical models for equipment and materials processes are based on the underlying physics and chemistry whenever such insight is available. This approach enables broad applicability and extrapolation of equipment and process parameters for the system. For issues involving high complexity (e.g., three-dimensional (3-D) flow dynamics), a reduced-order model is constructed and incorporated in order to complete the system-level description. Where neither is available, empirical models may be used (e.g., response surfaces or look-up tables). But in all cases the emphasis is on completing a *system-level dynamic* description.

The simulator elements corresponding to each aspect of the system are constructed using a Windows-based program. They are integrated through a process recipe simulator which defines overall process conditions and a sequence of actions as a function of time for the equipment to achieve these conditions. Process and equipment parameters are evaluated at each iteration step based on the gas flow and heat flow status, which in turn is determined by the process recipe simulator. The time dependent response of the equipment and process parameters are then a direct output of the simulation, allowing dynamic analysis of the overall process. The simulation results can be compared to experimental measurements for model validation, for process performance analysis, for fault detection and classification, and for process control. An experimentally validated simulator will aid significantly in new equipment design, process extrapolation to new parameter regimes, process optimization for manufacturing and environmental metrics, and design of new process control strategies.

In this paper, we will *demonstrate* the process of constructing a dynamic simulator for a polysilicon RTCVD process. We will first define the system to be simulated and find a mathematical representation for each physical element, thereby describing the various aspects of the system. We will then construct and validate a complete simulator for the polysilicon RTCVD process, and finally use the simulator for process optimization and other applications. The use of a Windows-based software for constructing dynamic simulators proves to be an important approach since we as scientists and engineers

can focus on the physics rather than the software of the simulation.

## II. MODEL ARCHITECTURE AND INTEGRATION

### A. Equipment Description

The rapid thermal chemical vapor deposition (RTCVD) system investigated by simulation in this paper is part of a multi-chamber cluster tool which integrates a rapid thermal processing module (RTCVD), a remote plasma processing module, and a wafer cleaning and surface analysis module [4]. The RTCVD module consists of a gas handling system [gas cylinder and mass flow controller (MFC)], the RTCVD reactor (including reactor chamber, heating lamps, and pyrometry sensor), reactor pumping station, equipment control system, and a two-stage differentially-pumped quadrupole mass spectrometry (QMS) sampling system. Fig. 1 presents a schematic representation of the RTCVD system. The reaction source gas for polysilicon RTCVD is a mixture of 10%  $\text{SiH}_4$  in Ar carrier gas. The pressure in the reactor chamber is measured using a capacitance manometer. The pressure during deposition is controlled using a feedback loop to continuously adjust the throttle valve position on the reactor pumping station while maintaining constant gas flow into the reactor. The wafer temperature is measured with a pyrometer operating at 5  $\mu\text{m}$  wavelength and is controlled using a feedback loop to regulate the power supply to the heating lamps. The design of the QMS sampling system permits active chemical sensing of the downstream gas composition (partial pressures) [5]. The consumption of reactants and the production of gaseous reaction products can be quantitatively monitored throughout the entire deposition process with a temporal resolution of approximately 1 s. Using this QMS system, process metrology (for film thickness) and equipment status diagnostics have been performed successfully for polysilicon RTCVD from  $\text{SiH}_4$  [6].

The RTCVD equipment is modeled in three sections: the gas handling system, the RTCVD reactor, and QMS sampling system. For each equipment section, three aspects are considered: the gas flow, the heat transfer, and the chemical reaction kinetics. The individual model elements for equipment and process are integrated through the mass balance and energy conservation equations for the entire system. The system-level dynamic simulation is accomplished through implementation of a process recipe, which defines the process conditions and a sequence of actions for the equipment to establish these conditions. Details of the models will be presented in the subsequent sections.

### B. Simulation Software

To illustrate the special features of our dynamic simulation technique, we present in Fig. 2 an overview of the equipment system simulator as constructed using a PC Windows-based simulation program [3]. The software uses a graphical user interface (GUI) to represent mathematical transformations. This allows the user to wire a block-diagram that connects various mathematical functionalities. One or more such diagrams can

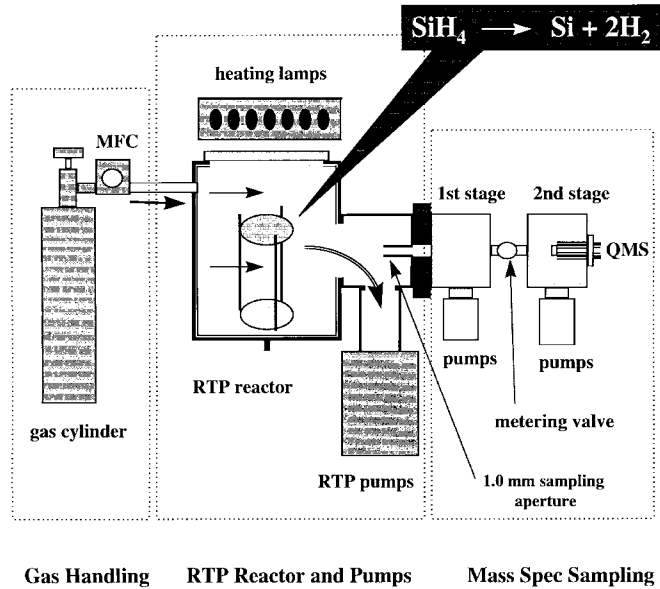


Fig. 1. Schematic representation of RTCVD module including gas handling, RTCVD reactor and pumping, and two-stage differentially pumped mass spectrometer system. The wafer is shown at the center of the reactor, where the silane decomposition reaction leads to Si film deposition.

be constructed to represent a physical model without having to write computer program codes.

The various computational functions are grouped into a hierarchical array of compound blocks, shown as shaded blocks in Fig. 2, according to the layout of the physical equipment (gas handling, RTP reactor and pumps, and mass spectrometer sampling system). Each compound block calculates a specific system parameter such as partial pressure, wafer temperature, surface reaction rate, and film thickness, etc. Hierarchical structure is achieved through multilevel compound block structures so that one can immediately identify the role of each group of calculations. Fig. 2 illustrates the structure of a multi-level compound block for the "RTP Reactor." In the first level, the simulator is structured to compute the  $\text{SiH}_4$  partial pressure by taking into account the " $\text{SiH}_4$ \_introduced" into the reactor, " $\text{SiH}_4$ \_pumped\_out" of the reactor, and " $\text{SiH}_4$ \_reacted" due to deposition on the wafer. The second level compound blocks then calculate the value for each of the above contributions. In Fig. 2, only the compound block for " $\text{SiH}_4$ \_reacted" is illustrated. There are eight levels of compound structure and over 1200 functional blocks in the RTCVD simulator presented here.

### C. General Model Structure

The dynamic simulator for polysilicon RTCVD is composed of five simulator elements: Process Recipe, Equipment Simulator, Sensors and Control System, Process Simulator, and Manufacturing Figures-of-Merit (FoM) Simulator. The role of each simulator and their correlation are presented below.

The Process Recipe simulator defines the status of the valves, the mass flow controllers (MFC's), the power input to the heating lamps as a function of time, and the overall process conditions (such as process pressure and temperature) and process timing. These parameters are used as input in the

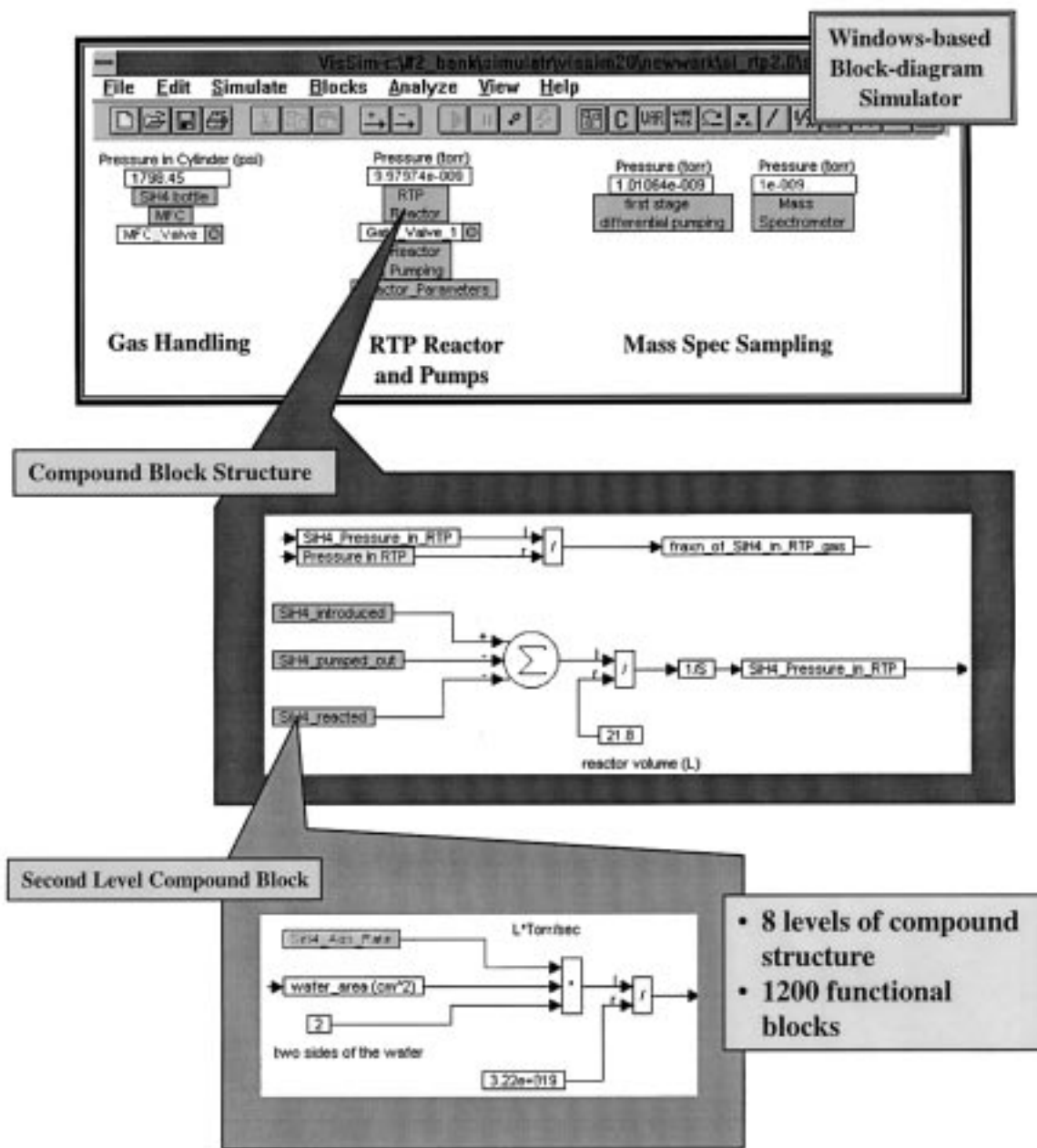


Fig. 2. Structure of Windows-based simulator for polySi RTCVD. The top panel is the top level Window of the RTCVD equipment simulator. In the middle expansion panel is a compound block for calculating SiH<sub>4</sub> partial pressure within the RTCVD reactor. The bottom expansion panel illustrates a second level compound block for calculating the SiH<sub>4</sub> partial pressure change induced by surface reactions. The complete RTCVD simulator consists of 8 levels of compound structure and about 1200 functional blocks.

Equipment Simulator, which then compute the status of the gas flow and heat flow, and as input in the Sensors and Control System to regulate the equipment status.

The Equipment Simulator uses the status of the valves, the MFC's, and the lamps defined in the process recipe to calculate the gas and heat flow conditions. The gas flow condition is determined by the chamber geometry, the mass flow rate, the pump and valve throughputs, etc. The output of the gas flow calculation is the total pressure and partial pressures in each section of the equipment (i.e., gas cylinder, reactor chamber, and QMS chambers). The heat flow condition is determined by the lamp radiation power, the wafer optical properties

(both absorptivity and emissivity change continuously during a deposition process due to the continuous variation of film structure), temperature control system, etc. The output of the heat flow calculation is the wafer temperature (and the wafer absorptivity and emissivity).

The Sensors and Control System simulator reads in the pressures and temperatures calculated in the Equipment Simulator and compares these values with the process pressure and process temperature as preset in the Process Recipe. The differences are input to PID (proportional, integral, and derivative) controllers to vary the throttle valve position for pressure regulation and to vary the lamp power for wafer

temperature control. The Control System also initiates and terminates gas flow and lamp power according to the overall process timing as defined in the Process Recipe. Therefore, the role of the Sensors and Control System simulator is to detect and regulate the gas flow and heat flow conditions so that the desired nominal process pressure and temperature can be established. Note, however, that the overall simulator captures the time-dependent changes in physical parameters throughout the entire process cycle, including those transients required to establish and remove nominal conditions.

The Process Simulator calculates the surface reaction kinetics and the resulting film deposition rates based on the reactant partial pressure and the wafer surface temperature as computed in the Equipment Simulator. Depending on the reaction temperature and pressure, the reaction and deposition rates can be limited either by the gas-phase transport/diffusion or by the surface reaction. Integration of reaction rates over time will give the values for total film thickness, the total reactant consumption, and the total gas product formation.

The Manufacturing FoM Simulator computes various manufacturing and environmental metrics from the output of the Process Simulator. Some issues of significance from a manufacturing point of view are process cycle time, consumables volume, product quality and reliability, and process yield, etc. Related environmental metrics are gaseous emission (gas phase products and un-reacted reactants), reactant utilization efficiency, and solid waste generation. Therefore, the complete dynamic simulator gives an overall assessment of the RTCVD process, from equipment status and control to manufacturability.

#### D. Gas Flow Conditions

The calculation of gas flow conditions is based on the mass balance in each piece of equipment. The total number of molecules input to each chamber must equal the sum of molecules remaining in the chamber, reacted on the surface, and pumped out through all pumping ports. The mathematical expression for the total pressure is

$$P_{\text{init}} + \int_0^t \frac{Q_{\text{MFC}} - Q_{\text{aperture}} - Q_{\text{gate-valve}} + Q_{\text{reaction}}}{V_{\text{chamber}}} dt = P_{\text{total}}$$

where  $P_{\text{init}}$  is the base pressure of the reactor in Torr;  $Q_{\text{MFC}}$  is the total throughput in Torr-liter/s from the mass flow controller into the RTCVD reactor;  $Q_{\text{aperture}}$  is the throughput in Torr-liter/s through the sampling aperture from the RTCVD reactor out to the first stage QMS sampling chamber;  $Q_{\text{gate-valve}}$  is the throughput in Torr-liter/s through the gate valve and throttle valve from the RTCVD reactor out to the pumping station;  $Q_{\text{reaction}}$  is the throughput change due to surface and gas phase chemical reactions;  $V_{\text{chamber}}$  is the chamber volume in liters; and  $P_{\text{total}}$  is the total pressure in RTCVD reactor. In this calculation, the number of molecules for reactant, carrier gas, and product are all included; and therefore, the resulting pressure is the total pressure in the reactor.

The gas pressure calculations do not include flow dynamics modeling, and they assume perfect mixing between all gas molecules. This reduced-order model significantly simplifies the computation, and proves to be a good approximation to the gas flow behavior as will be shown in Section III-B. However, further improvement to include more complex gas flow dynamics will be necessary where more subtle aspects of deposition kinetics and equipment state are to be elucidated.

#### E. Heat Flow Conditions

In RTCVD modeling studies, the calculation of wafer temperature has attracted most of the research effort. Various physical, semi-empirical, and empirical models have been developed for computing heat transfer processes that may affect the wafer temperature [7]. In our simulator, a considerably simpler heat flow representation is adopted in order to enable its integration with the numerous other elements required to describe manufacturing and environmental metrics. The energy balance for the wafer consists of the lamp radiation absorbed by the wafer, the power radiated by the wafer, the power lost through conductive and convective heat transfer, and the energy transfers associated with dynamic power changes through the process cycle. This can also be expressed (in Watts) as the following:

$$aQA - 2eA\sigma T_w^4 - W_{cc} = mC_p \frac{dT_w}{dt}$$

where the first term in the equation corresponds to the power absorbed by the wafer, the second term is the power radiated by the wafer, the third term is the power lost through other channels, and the fourth term is the power consumed for heating the wafer;  $a$  is the wafer absorptivity;  $Q$  is the incoming lamp radiation flux on the wafer;  $A$  is the wafer surface area;  $e$  is the wafer emissivity;  $\sigma$  is the Stefan-Boltzmann constant;  $T_w$  is the wafer temperature;  $W_{cc}$  is the total conductive and convective heat loss;  $m$  is the mass of the wafer;  $C_p$  is the specific heat of the wafer material;  $\frac{dT_w}{dt}$  is the heating rate of the wafer; the wafer temperature is computed by integrating the wafer heating rate over time:  $T_w = T_{\text{init}} + \int \left\{ \frac{dT_w}{dt} \right\} dt$ , where  $T_{\text{init}}$  is the initial wafer temperature.  $W_{cc}$  is modeled in our simulator as a linear function of the difference between the wafer temperature and the ambient temperature, i.e.,

$$W_{cc} = f(T_{\text{wafer}} - T_{\text{ambient}}).$$

The absorptivity of the wafer is strongly dependent on the film thickness and structure (single or multiple layers of different films) on the wafer, the spectral distribution of the heating lamp [8], and the wafer temperature at any point in the process cycle. The total wafer emissivity is dependent on the wafer temperature and the film structure and thickness. During a RTCVD process, the wafer temperature varies continuously with time. The film on the wafer surface increases in thickness during deposition. The spectral distribution of the lamp radiation also changes dramatically because of the lamp temperature variation caused by lamp power regulations. Reduced-order model was used in the computation of “wafer absorptivity” and “wafer emissivity” based on physical models developed by Y. Sorrell and coworkers [9].

Model reduction was accomplished by first running a program written by Y. Sorrell *et al.* [9] to establish a database for wafer absorptivity and emissivity. This database was curve-fitted for three variable parameters: film thickness, wafer temperature, and lamp temperature. The resulting mathematical expression was then used to construct a block-diagram which uses film thickness, wafer temperature, and lamp temperature as input. All three parameters vary continuously during a RTCVD process, and therefore the wafer absorptivity and emissivity were computed at each iteration time step.

#### F. Chemical Kinetics

While the gas flow model establishes partial pressures in the RTCVD reactor, the heat flow model computes the temperature of the wafer. These two parameters comprise the base for evaluating the chemical kinetics of surface reactions which lead to polysilicon film deposition. Due to the cold wall configuration of the RTCVD reactor and the relatively low temperatures (550–750 °C) for polysilicon deposition, the contribution of gas phase reaction is neglected in our simulator. The film growth rate and total film thickness can be calculated from the kinetics of three surface reactions: SiH<sub>4</sub> adsorption, SiH<sub>x</sub> decomposition (where  $x = 1-3$ ), and hydrogen desorption. The surface rate expressions and film growth rate are shown at the bottom of the page.

The adsorption of each SiH<sub>4</sub> molecule requires two surface active sites (surface dangling bonds, \*) and results in one adsorbed SiH<sub>3</sub> group and one adsorbed H atom. A surface site is considered active for adsorption and reaction if it is not occupied by a SiH<sub>x</sub> group or H atom. In the adsorption rate expression,  $R_{\text{ads}}$  is the rate for SiH<sub>4</sub> adsorption,  $S_0(T)$  is the effective initial (i.e., on clean Si surface) sticking probability and is temperature-dependent [11],  $F_{\text{SiH}_4}$  is the SiH<sub>4</sub> flux reaching the surface, and  $\theta_*$  is the coverage (fractions of a monolayer) of surface active sites. The surface flux of SiH<sub>4</sub> may be different from that in the bulk gas phase if the surface reaction rate is high enough to induce a concentration gradient near the surface. A boundary layer model was therefore constructed to account for the thermal diffusion rate from the gas bulk to the near-surface region.

The decomposition of an adsorbed SiH<sub>3</sub> species requires two active sites, and produces three adsorbed H atoms. In the decomposition rate expression,  $R_{\text{SiH}_3}^-$  is the rate of SiH<sub>3</sub>

decomposition,  $k_2$  is the rate constant, and  $\theta_{\text{SiH}_3}$  is the surface coverage of SiH<sub>3</sub> groups. Since the decomposition of the surface SiH<sub>x</sub> is not rate-limiting, details of this step are not crucial, and we assume  $\text{SiH}_3 + 2_* \rightarrow \text{SiH} + 2\text{H}$  for convenience.

The desorption of each H<sub>2</sub> molecule consumes two adsorbed H atoms, and creates two surface active sites. In the first-order desorption rate expression [12],  $\gamma$  is the pre-exponential factor,  $E_a$  is the activation energy,  $k$  is the Boltzmann constant,  $T$  is the surface temperature, and  $\theta_{\text{H}}$  is the surface coverage of adsorbed atomic H. The surface H coverage can be calculated by integrating over time the rates of all the reaction steps that produce or consume H, as illustrated in Fig. 7. Similarly, the surface coverage of SiH<sub>3</sub> and active surface sites were computed at each iteration step.

#### G. Growth Rate and Total Film Thickness

For the adsorption and surface decomposition of each SiH<sub>4</sub> molecule, a Si atom is deposited on the surface and two H<sub>2</sub> molecules are released to the gas phase. Therefore, the net deposition rate,  $R_{\text{growth}}$ , is equal to the SiH<sub>4</sub> adsorption rate,  $R_{\text{ads}}$ . Because the surface temperature and the SiH<sub>4</sub> partial pressure change continuously over a deposition process, the film growth rate ( $R_{\text{growth}}$ ) is also time-dependent. The total film thickness deposited is the time integration of the growth rate, and subsequently depends on the history of the deposition process.

The overall deposition kinetics can be transport-limited or desorption-limited, depending on the temperature and pressure of the deposition [13]. At sufficiently high surface temperature, the H<sub>2</sub> desorption rate is high enough to efficiently remove adsorbed H from the surface so that the coverage of active sites ( $\theta_*$ ) is approaching unity. Then, the growth rate ( $R_{\text{growth}} = R_{\text{ads}}$ ) is limited by how fast SiH<sub>4</sub> molecules diffuse through the boundary layer and impinge onto the surface ( $F_{\text{SiH}_4}$ ). Processes in this regime are therefore transport-limited. If the deposition occurs at a relatively lower surface temperature, H<sub>2</sub> desorption is slow, resulting in surface H accumulation. High surface H coverage reduces the number of reactive sites available for further SiH<sub>4</sub> adsorption, and limits the subsequent Si deposition rate. In this case, the deposition kinetics is hydrogen desorption-limited. The dynamic simulation provides time-dependent results for surface concentrations throughout the process cycle.

---

SiH <sub>4</sub> Adsorption:	$\text{SiH}_4 + 2_* \Rightarrow \text{SiH}_3 + \text{H}$	$R_{\text{ads}} = S_0(T)F_{\text{SiH}_4}\theta_*^2$
SiH <sub>x</sub> Decomposition:	$\text{SiH}_3 + 2_* \Rightarrow \text{SiH} + 2\text{H}$	$R_{\text{SiH}_3}^- = k_2\theta_{\text{SiH}_3}\theta_*^2$
H <sub>2</sub> Desorption:	$2\text{H} \Rightarrow \text{H}_2 + 2_*$	$R_{\text{H}_2} = (\gamma e^{-E_a/kT})\theta_{\text{H}}$
Surface H Coverage:	$\theta_{\text{H}} = \int (R_{\text{ads}} + 3R_{\text{SiH}_3}^- + 2R_{\text{H}_2}) dt$	
Si Film Growth Rate:	$R_{\text{growth}} = R_{\text{ads}}$	
Film Thickness:	$\text{Film Thickness} = \int R_{\text{growth}} dt$	

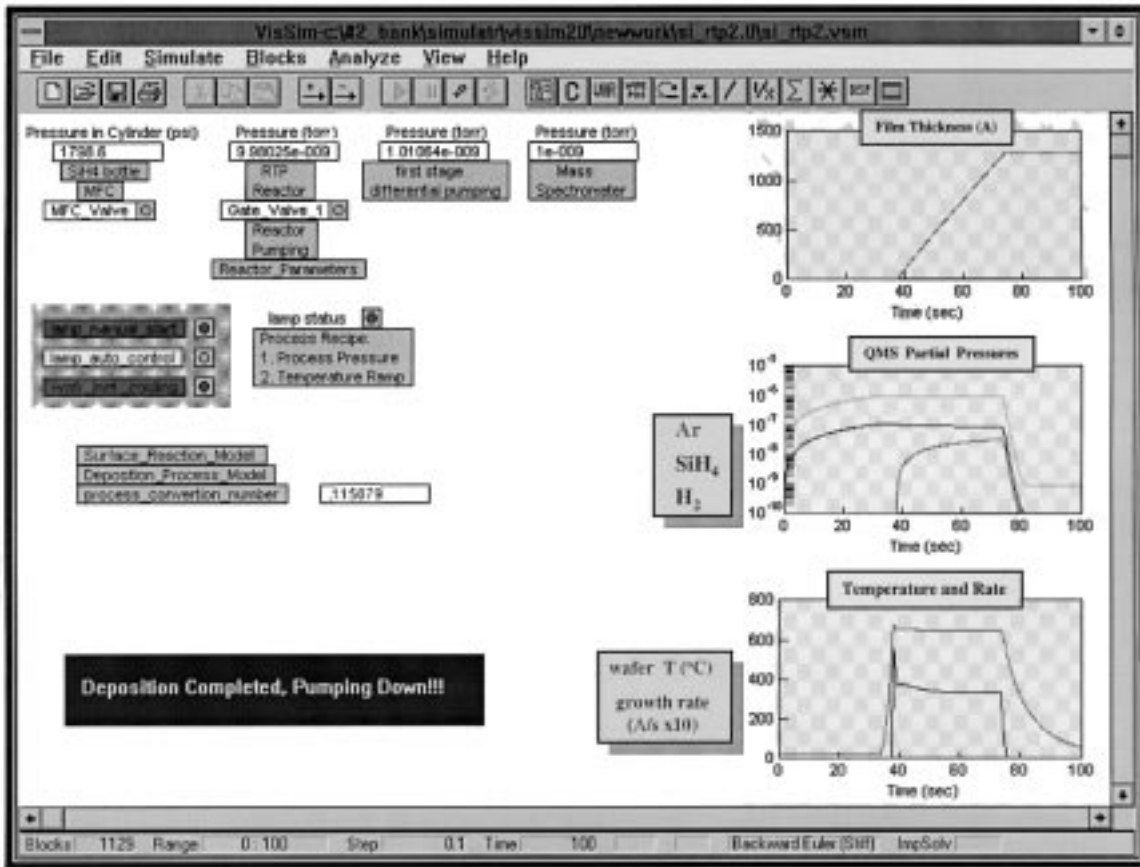


Fig. 3. Windows view of the RTCVD simulator. From top to bottom on the left-hand side of the window are the equipment simulator, the process recipe and control simulator, the deposition kinetics simulator, and a display panel for overall process status. The three plots on the right-hand side are simulation outputs for film thickness (top), QMS partial pressure signals (middle), and wafer temperature and growth rate (bottom).

#### H. Model Integration and Dynamic Simulation

In order to achieve a system-level description for the overall RTCVD process, the various model elements for gas flow, heat transfer, and chemical reactions must be incorporated into one integrated simulator. This allows for a coherent investigation of all system parameters as a function of time. We used globally defined variable parameters in each simulator element so that only one value is computed and assigned for each parameter at each iteration step. For example, the wafer temperature is computed in the heat transfer model, and this value is passed elsewhere in the simulator for use in other elements to further calculate the surface reaction rate, the conductive and convective heat loss, the wafer absorptivity, and the wafer emissivity. Fig. 3 shows a Windows view of the complete simulator for polysilicon RTCVD. In the left half of the window, from top to bottom are the equipment simulator (as seen in Fig. 2), the process recipe and process control simulator, the deposition kinetics models, and a display panel for the system status. On the right side of the window are plots for the film thickness (top panel), the QMS partial pressure signals for Ar, SiH<sub>4</sub>, and H<sub>2</sub> (middle panel), and the wafer temperature and the growth rate (bottom panel).

To simulate a deposition process, a number of process parameters must be entered from the Process Recipe panel. Numerical values can be defined for the mass flow rate, process pressure, process time, process temperature, and process tim-

ing. Once the simulation is initiated, the Control System Simulator will implement a series of actions for the MFC, the throttle valve, and the lamp power supply in order to 1) bring the total pressure in the reactor to 5.0 Torr using a constant mass flow rate of 300 sccm; 2) rapidly heat the wafer to 650 °C; 3) maintain the reactor at 5.0 Torr and the wafer at 650 °C for 30 s; and 4) finally terminate both gas flow and wafer heating, and simultaneously evacuate the reactor. PID (proportional, integral, and derivative) controls are used to regulate the total pressure and wafer temperature. The difference between the measured pressure and the preset pressure is input to the PID pressure simulator to define the exact position of the throttle valve. Similarly, the actual wafer temperature is compared to the preset process temperature for PID control on the power supply to the heating lamp.

At each iteration step, the SiH<sub>4</sub> partial pressure and the wafer temperature are evaluated, and their values are used to compute the surface reaction and film growth rates. During a simulation, all system parameters can be tabulated or plotted for dynamic analysis of equipment, process, materials consequences, sensor response, and the control system behavior.

### III. EXPERIMENTAL VALIDATION

#### A. CVD Reaction Kinetics

Extensive effort has been devoted to independently validate the various model elements in the RTCVD simulator. The

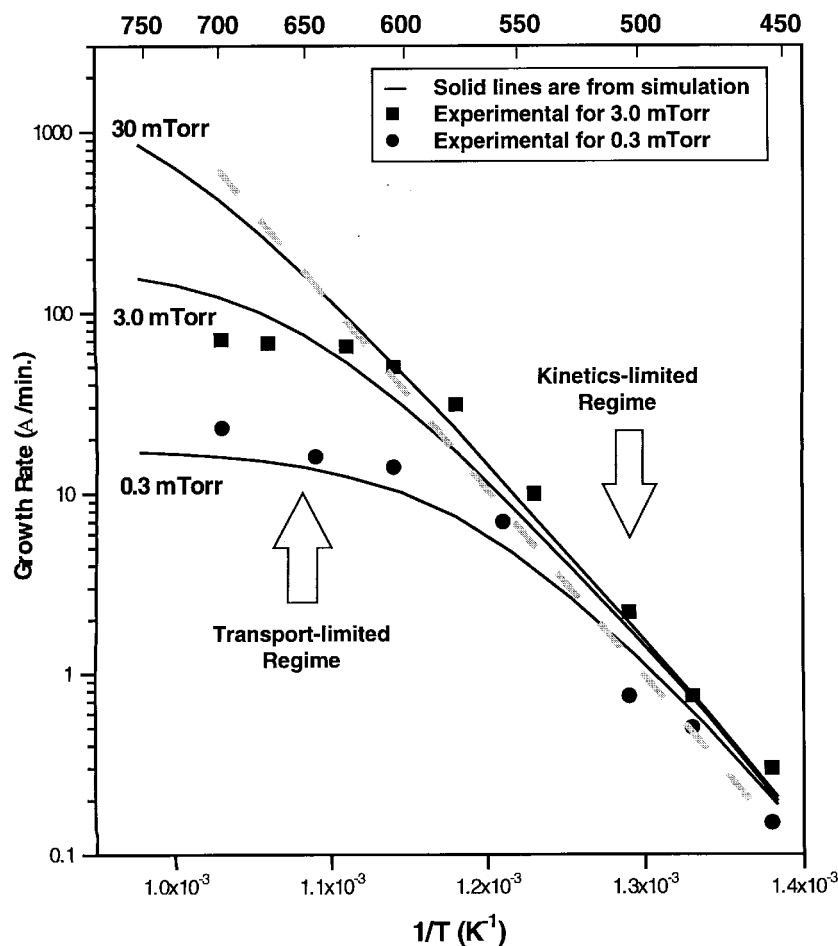


Fig. 4. Arrhenius plots of simulated polysilicon growth rate (as a function of  $1/T(K)$ ) at various  $\text{SiH}_4$  partial pressures. The transition from the surface reaction limited regime to the transport-limited regime is clearly observed from our simulation and is consistent with experimental results [13].

simulation results for chemical kinetics, equipment dynamics, and overall process dynamics have been compared to available experimental data, as demonstrated in this section and Sections III-B and III-C.

Fig. 4 presents simulation results for the polysilicon RTCVD deposition rate as a function of surface temperature at various  $\text{SiH}_4$  partial pressures. For the 0.3 mTorr  $\text{SiH}_4$  deposition process, the growth rate exhibits a strong temperature dependence under 500 °C with an activation energy of  $\sim 45$  kcal/mole, very close to that for hydrogen desorption at 46 kcal/mole; here, the deposition process is rate-limited by surface hydrogen desorption. With increasing temperature above 550 °C, the deposition rate is less temperature-dependent; in this regime, the transport of  $\text{SiH}_4$  molecules to the wafer surface becomes a rate-limiting factor. With increase of  $\text{SiH}_4$  partial pressure, the deposition rate in the transport-limited regime becomes higher due to the larger  $\text{SiH}_4$  flux. The transition from the reaction-limited regime to the transport-limited regime also shifts to higher temperatures because of the increasing surface H coverage at higher  $\text{SiH}_4$  partial pressures. This behavior has been experimentally observed, and our simulation results are in relatively good agreement with the experimentally measured deposition rates under various conditions [13].

### B. Equipment Dynamics: Partial Pressures

In order to evaluate the accuracy of our equipment model, the partial pressures of reactant ( $\text{SiH}_4$ ), carrier gas (Ar), and product ( $\text{H}_2$ ) in the reactor as well as in the mass spectrometer chambers were simulated as a function of time throughout the deposition process cycle. In Fig. 5, the simulation results for Ar and  $\text{H}_2$  (solid lines) are compared to our experimentally measured mass spectrometer signals (solid or open circles). The Ar signal provides evidence of when the gas flow was initiated (at  $\sim 15$  s), process pressure was reached (at  $\sim 45$  s), and gas flow was terminated (at  $\sim 100$  s). The  $\text{H}_2$  signal indicates when surface reaction was initiated to produce  $\text{H}_2$  and when the system pump-down began at the end of the deposition process. The trends in Fig. 5 clearly show that the simulation result is in good agreement with experimental measurements.

The effect of gas flow rate on the partial pressures can also be quantitatively predicted using our dynamic simulator. Fig. 6 compares simulation (solid line) and experimental data (points) for the QMS signal of  $\text{H}_2$  during a deposition process using 750 °C, 5 Torr (10%  $\text{SiH}_4/\text{Ar}$ ), for 40 s. An increase in flow rate (200, 500, and 1000 sccm) caused the  $\text{H}_2$  signal measured by QMS to decrease significantly. The simulation

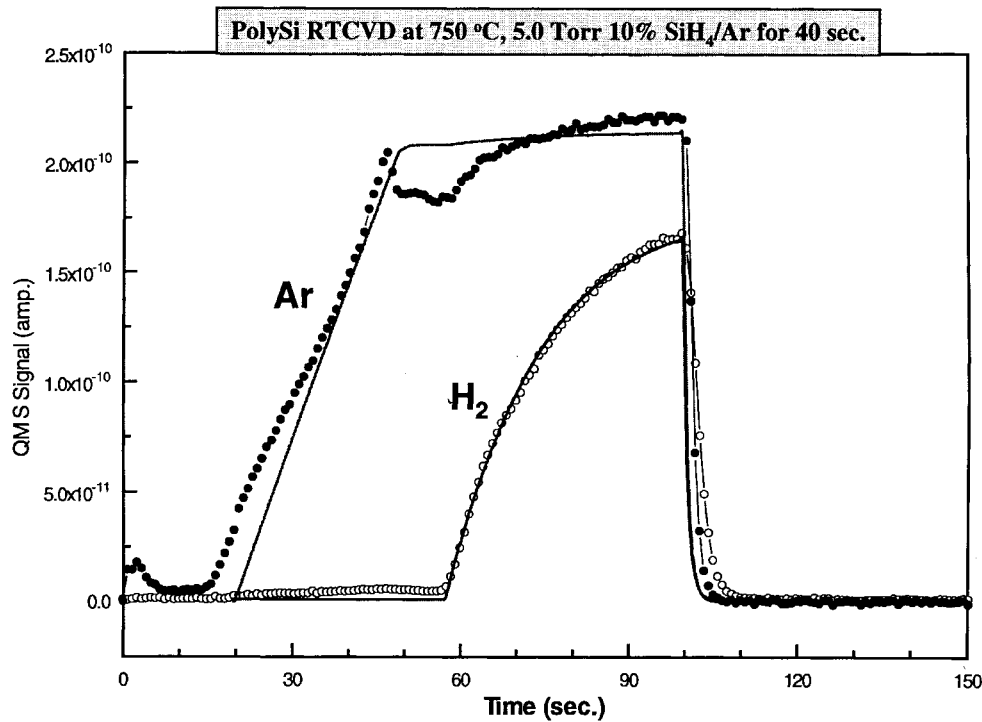


Fig. 5. QMS signals (ion current) for Ar and  $H_2$  throughout the whole process cycle for polysilicon RTCVD at  $750^\circ\text{C}$  and 5.0 Torr 10%  $\text{SiH}_4/\text{Ar}$  for 40 s. The circle data points are from actual experimental measurements, and the solid lines are from simulation.

accurately predicts this change in  $H_2$  partial pressure. For each flow rate, the line-shape of the simulated  $H_2$  signal as a function of time is in excellent agreement with that from the experimental measurement. The small deviation of experimental data from simulation for the 1000 sccm process was due to a malfunction in the temperature control system during that particular experimental run. The above results suggest that the physical models in our simulator correctly describe the equipment behavior. The strong dependence of QMS  $H_2$  signal on flow rate can be understood (with the help of the simulator) as arising from changing residence time for the  $H_2$  reaction product generated within the reactor as a function of flow rate.

### C. Overall Process Dynamics

The accuracy of the simulation in describing the overall system behavior can be evaluated through the prediction of total film thickness for the implementation of a process recipe. Fig. 7 presents a correlation plot of the deposited film thickness from simulation and experiment. The experimental thickness was determined by averaging five points across the wafer radius based on ellipsometry measurements after each polysilicon deposition [6] on 27 wafers, using varying process time and temperature ( $600\text{--}850^\circ\text{C}$ ). The simulated thickness assumes perfect uniformity across the entire wafer. If the simulation precisely predicted the deposited film thickness for these experiments, all data points would fall on the diagonal line. The data distribution indicates that the overall agreement is reasonably good. The simulation slightly overestimates the deposition thickness in the low temperature regime, and underestimates the thickness in the higher temperature regime. This suggests that the simulator captures the physics and

chemistry of the system well to first order over a broad dynamic range, but that some systematic subtleties are not yet represented.

### D. Opportunities for Simulator Improvement

Given the high complexity of a process cycle, dynamic simulations offer substantial advantage for rapid learning of the process and equipment behavior. Complex system behavior can be described and predicted with reasonable accuracy over a broad dynamic range for various process parameters. In some cases, more sophisticated physical models may be needed to capture important aspects of dynamic behavior.

For instance, the gas flow model in our simulator assumed perfect mixing of all gases, so that no partial pressure gradient exists between the various locations in the reactor. This obviously does not reflect the actual gas flow pattern, and therefore may have contributed to the errors in predicting the film thickness presented in Fig. 7. A more accurate model should account for the  $\text{SiH}_4$  depletion downstream from the wafer due to fast reactions at the wafer surface. Similarly, improvement of simulation results could also benefit from more detailed models for conductive and convective heat loss, control system mechanisms, equipment components (MFC's, valves, pumps), and sensors. In addition, the materials quality issue and equipment aging effect have not been directly addressed in the current version of our simulator. We are in the process of incorporating into our simulator such factors as materials quality, conformality, across-wafer uniformity, and product yield.

Normally, it is expected that more complex models require higher computational power, bounding the value of such simulators. However, salient elements of more complex

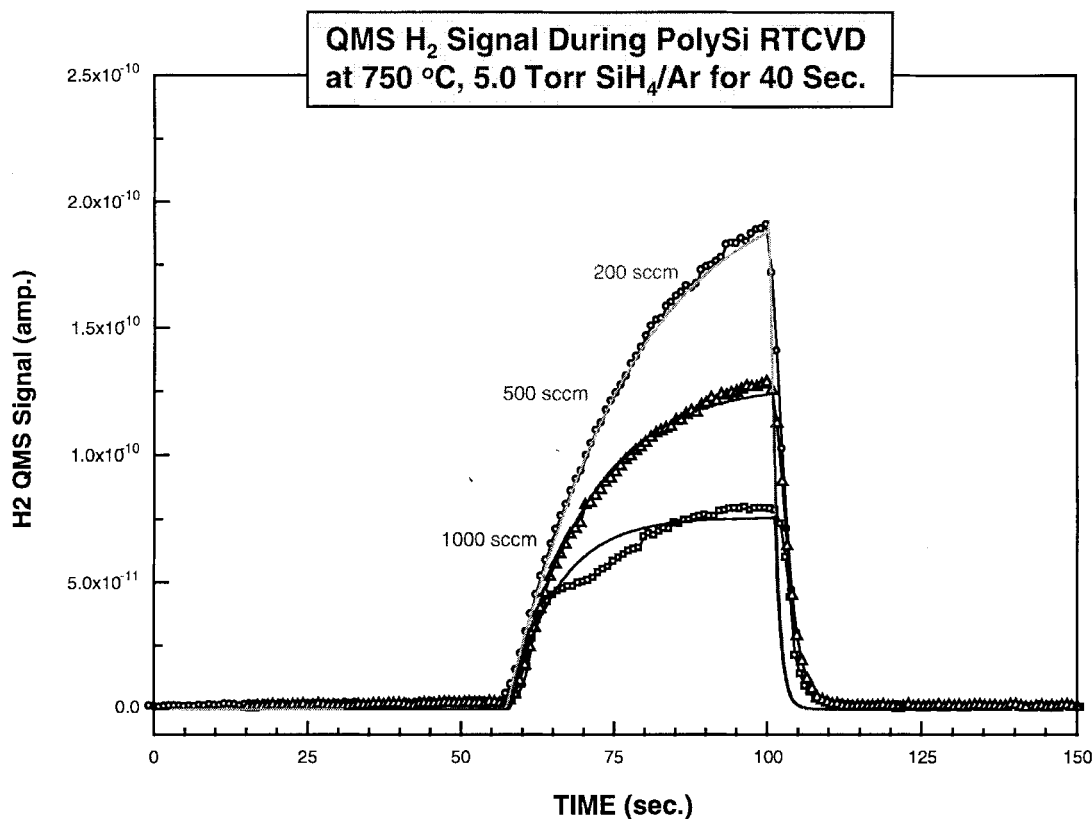


Fig. 6. Comparison of H<sub>2</sub> QMS signal during a deposition process for three different gas flow rates (200 sccm, 500 sccm, and 1000 sccm). The solid lines are from simulation and the data points are experimental measurements.

physical/chemical behavior may be captured through far more comprehensive and sophisticated modeling studies and the generation of reduced-order (compact) models from them for direct incorporation into the simulator. An example of this was given for the case of reduced-order absorptivity/emissivity models in Section II-E. The use of reduced-order models (compatible with dynamic system-level simulators) incurs the higher cost of sophisticated computational studies and compact model generation, but benefits from greater insight and accuracy of the reduced-order models.

#### IV. APPLICATIONS AND EXTENSIBILITY OF DYNAMIC SIMULATORS

##### A. Process and Equipment Design

An immediate application of an experimentally validated simulator is to generate improved process recipes or equipment designs. Physically-based models are generally valid over a broad dynamic range, providing descriptions of the process and equipment behavior in new, uncharted parameter regimes where sufficient sets of experiments may be tedious. In such situations, simulation may be effectively employed to sample and understand new parameter regimes and thereby define much smaller, better focused sets of experiments. This will certainly decrease process learning time by reducing the number of experiments required to qualify new process/equipment designs.

Within a well established process regime, an experimentally validated simulator can predict with reasonable accuracy the deposited film thickness for a given process recipe. Conversely, the exact values for process parameters (such as process time, temperature, and pressure) can be determined from a simulation to achieve a specific film thickness. The RTCVD simulator described in this paper has been frequently and successfully used to define process conditions for film depositions of desired thickness [14].

##### B. Process/Equipment Diagnostics and Fault Detection

A dynamic simulation can directly generate the time-dependence of all process and equipment parameters throughout the entire process cycle, and can therefore be used as a benchmark for evaluating the performance of a system, i.e., the values for a “perfect” run when the equipment and the process perform normally. If the experimental sensor signals deviate from that of the simulation, fault detection has been accomplished.

The H<sub>2</sub> QMS signal for the 1000 sccm deposition process in Fig. 6 presents an excellent example for this type of diagnostics and fault detection. In that case, the experimental H<sub>2</sub> signal did not rise to the level as expected from the simulation. The wafer temperature was not increased to 750 °C as programmed, but stalled at 725 °C for 10 s before further heating to 750 °C. This deviation was later determined to be caused by a malfunction in the temperature control system.

Furthermore, dynamic simulation could significantly aid in classifying as well as detecting system faults. Various possible

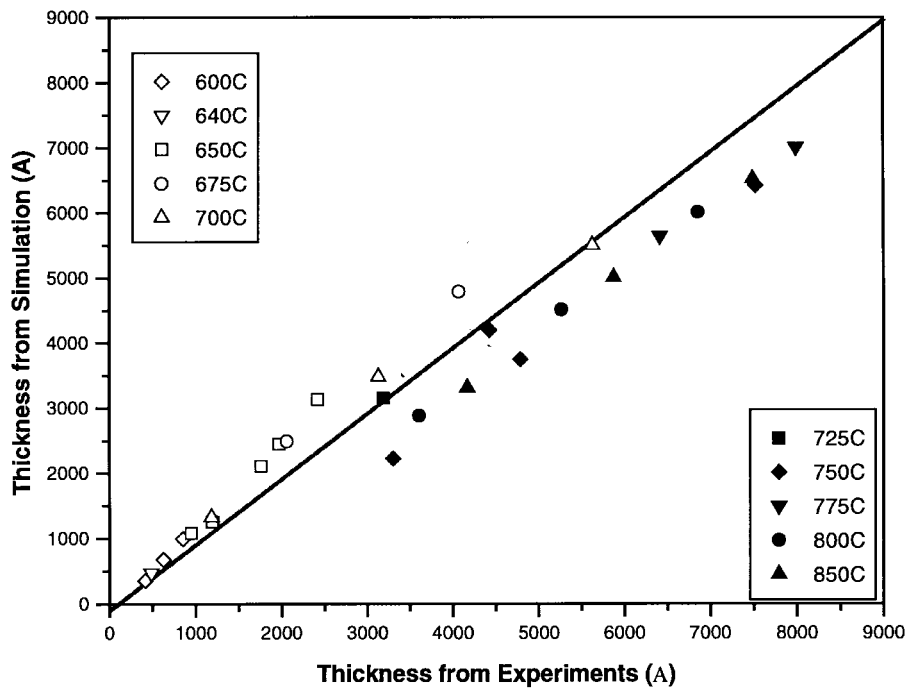


Fig. 7. Correlation plot of simulated and experimental film thickness for 27 deposition processes of polySi from  $\text{SiH}_4$ .

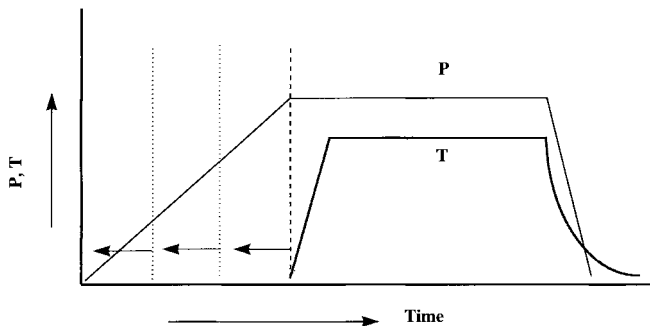


Fig. 8. Virtual experiment design for process optimization. The time-sequence of pressure ( $P$ ) and temperature ( $T$ ) ramps is schematically represented for a conventional process. Early heating is illustrated as advancing the heating initiation to positions indicated by the dotted lines.

system faults can be simulated using dynamic simulation, and their characteristics can be documented for diagnosing process and equipment status. This may provide the basis for effective process control, either through advisory information coupled with operator/engineer intervention, or through run-to-run or real-time control.

### C. Process Optimization for Manufacturing and Environmental Metrics

Dynamic simulation exercises can be performed to evaluate numerous manufacturing and environmental metrics such as process cycle time, reactant utilization efficiency, consumables volume, and product quality, thereby achieving manufacturing-relevant process optimization. Dynamic simulations provide better controls on all the parameters that may affect these metrics and minimize time- and resource-consuming experimental

work. In the example below, a process for growing 2000 Å polysilicon is optimized for process cycle time and reactant utilization efficiency by varying the process temperature and the event timing.

The virtual experiment is designed to grow a 2000 Å film in a 5 Torr process gas which contains 10%  $\text{SiH}_4$  in an Ar carrier. The conventional process sequence includes the establishment of process pressure (5.0 Torr) with a constant gas flow rate (e.g., 300 sccm), followed by a heating ramp to the process temperature. The wafer temperature is kept constant at the process temperature (650–750 °C, in the range where acceptable material quality is achieved) until 2000 Å of polysilicon is deposited on the surface. Gas flow and lamp heating are terminated at the end of the deposition. Fig. 8 illustrates the time sequence of the pressure and temperature ramps. In the following discussions, process cycle time is defined as the time from the initial gas flow until the deposition is terminated by turning off heating and gas flow. The  $\text{SiH}_4$  utilization efficiency (or process conversion yield) is defined as the percentage of  $\text{SiH}_4$  molecules that are converted to polysilicon film with respect to the total number of  $\text{SiH}_4$  molecules input to the RTCVD reactor over the entire process cycle. Shorter process cycle times are preferred for increased manufacturing throughput (and therefore productivity). A higher conversion yield is preferred to reduce both the manufacturing consumables cost and the environmental penalty associated with waste of reactants.

If the wafer heating is initiated at an earlier time (e.g.,  $P = 3.0$  Torr or 1.5 Torr), as illustrated schematically in Fig. 8, both the overall  $\text{SiH}_4$  utilization efficiency and process cycle time are changed. In Fig. 9, the top and bottom panels show the  $\text{SiH}_4$  utilization efficiency and the process cycle time, respectively, for three process temperatures as a function of the

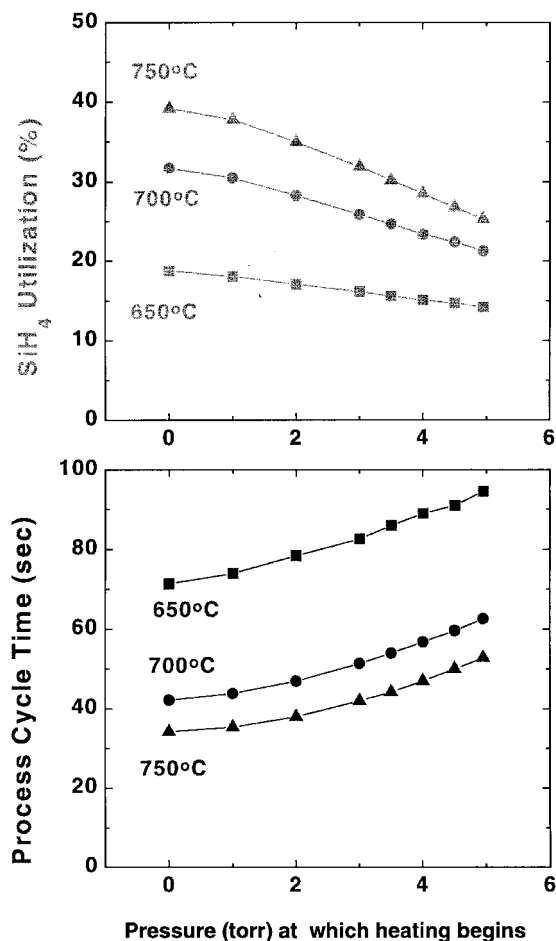


Fig. 9. Effect of process timing and process temperature on materials utilization efficiency (top panel) and process cycle time (bottom panel).

TABLE I  
MULTIVARIABLE AND COMPLEX CORRELATION BETWEEN SYSTEM PARAMETERS AND MANUFACTURING FIGURES-OF-MERIT

<p><b>Equipment and Process Parameters and Design:</b></p> <ul style="list-style-type: none"> <li>• Equipment design</li> <li>• Gas flow</li> <li>• Pressure</li> <li>• Temperature</li> <li>• Ramp rate (for temperature and pressure)</li> <li>• Process timing</li> <li>• Control parameters</li> </ul> <p><b>Manufacturing Figures-of-Merit (FoM's):</b></p> <ul style="list-style-type: none"> <li>• Product quality</li> <li>• Product Reliability</li> <li>• Throughput and cycle time</li> <li>• Consumables cost</li> <li>• Equipment cost of ownership</li> <li>• Environmental compliance</li> </ul>
---

pressure at which heating is initiated. A pressure of 5.0 Torr in the plots corresponds to wafer heating initiated after the 5.0 Torr process pressure is established, while a lower pressure corresponds to an earlier initiation of heating. At 0 Torr, wafer heating and gas flow are initiated simultaneously.

As shown in Fig. 9 for the 650 °C process, the process cycle time is reduced from 95 s to 71 s if the heating is initiated at 0 Torr instead of at 5 Torr, while the materials utilization efficiency is increased from 14.2% to 18.8%. As the process temperature is increased, the effect of this particular event timing becomes more significant. For the 750 °C process, both the process cycle time and the materials utilization efficiency are improved by over 50% by initiating heating and gas flow simultaneously (i.e., at 0 Torr). Regardless of the event timing, the temperature increase itself has an even greater effect: the temperature increase from 650 °C to 750 °C shortens the cycle time by a factor of two and enhances the utilization efficiency by two times of baseline. When event timing and wafer temperature are optimized, a total of three times improvement can be realized for each of the two manufacturing and environmental metrics.

An optimal process point impacts multiple manufacturing figures-of-merit as shown in Table I. Each one of those may be affected by any one or a combination of multiple equipment and process parameters. Experimental optimization of equipment and process parameters is typically costly and time-consuming, and requires a coherent analysis of multiple manufacturing and environmental figures-of-merit from a large number of combinations of parameters, each defining a single manufacturing process. Dynamic simulation provides a powerful tool to facilitate optimization of individual and multiple manufacturing metrics for complex time-dependent behavior. It may also provide a convenient vehicle to combine individual figures-of-merit for identifying an optimal design point from an overall cost function when tradeoffs must be made.

V. SUMMARY

We have demonstrated the formulation and construction of a physically-based dynamic simulator for the rapid thermal deposition of polysilicon from SiH<sub>4</sub>. Experimental validation indicates that the simulator captures the essential physics and chemistry of mass transport, heat transfer, and chemical kinetics of the RTCVD process as executed by equipment, sensor, and control systems. Reduced-order models are also employed to represent processes involving high complexity or poorly understood physics. Integration of individual simulator elements for equipment, process, sensors, and controls enables analysis of not only the deposition kinetics, but also a broad range of system properties including equipment performance, gas flow conditions, wafer temperature variation, wafer optical properties (absorptivity/emissivity), and gas composition in the reactor. The experimentally validated simulator can be used to optimize a process with respect to the total process cycle time, consumables volume, and reactant utilization. Dynamic simulation also aids significantly in equipment design, optimization, and fault detection and classification. This study clearly demonstrates that integrated, system-level simulation is a powerful tool for investigating the dynamic behavior of process and equipment parameters, for identifying optimal process points, and for assessing gains and tradeoffs between various manufacturing and environmental metrics.

## ACKNOWLEDGMENT

The authors thank Visual Solutions, Inc. for consultation on VisSim<sup>TM</sup>.

## REFERENCES

- [1] E. Sachs, G. H. Prueger, and R. Guerrieri, *IEEE Trans. Semiconduct. Manufact.*, vol. 5, p. 3, Feb. 1992.
- [2] G. Lu, M. Bora, and G. W. Rubloff, "Polysilicon RTCVD process optimization for environmentally-conscious manufacturing, *IEEE Trans. Semiconduct. Manufact.*, vol. 10, pp. 390-398, Aug. 1997.
- [3] S. Tazawa, S. Matsuo, and K. Saito, *IEEE Trans. Semiconduct. Manufact.*, vol. 5, no. 1, p. 27, 1992.
- [4] N. A. Masnari, J. R. Hauser, G. Lucovsky, D. M. Maher, R. J. Markunas, M. C. Ozturk, and J. J. Wortman, *Proc. IEEE*, vol. 81, p. 42, Mar. 1993.
- [5] L. L. Tedder, G. W. Rubloff, D. H. Kim, and G. N. Parsons, *J. Vac. Sci. Technol.*, vol. B13, no. 4, p. 1924, 1995.
- [6] L. L. Tedder, G. W. Rubloff, B. Conaghan, and G. N. Parsons, *J. Vac. Sci. Technol.*, vol. A14, no. 2, p. 267, 1996.
- [7] S. A. Campbell, in *Computational Modeling in Semiconductor Processing*, M. Meyyappan, Ed. Boston, MA: Artech House, 1995 p. 325, and references therein.
- [8] F. P. Incropera and D. P. DeWitt, *Fundamentals of Heat and Mass Transfer*, 3rd ed. New York: Wiley, 1990.
- [9] F. Y. Sorrell, and R.S. Gyurcsik, *IEEE Trans. Semiconduct. Manufact.*, vol. 6, pp. 273-276. Aug. 1993
- [10] S. Yu, Ph.D. dissertation, North Carolina State Univ., Raleigh, 1994.
- [11] J. M. Jasinski and S. M. Gates, *Acc. Chem. Res.*, vol. 24, pp. 9-14, 1991.
- [12] K. Sinniah, M. G. Sherman, L. B. Lewis, W. H. Weinberg, J. T. Yates Jr., and K. C. Janda, *J. Chem. Phys.*, vol. 92, no. 9, p. 5700, 1990.
- [13] M. Liehr, C. M. Greenlief, S. R. Kasi, and M. Offenber, *App. Phys. Lett.*, vol. 56, no. 7, p. 629, 1990.
- [14] L. L. Tedder and G. W. Rubloff, unpublished.



**Guangquan Lu** received the B.S. degree in chemistry in 1985 from Shandong University, China, and the Ph.D. degree in chemistry in 1992 from the University of California, San Diego.

He is an Engineer with Novellus Systems, Inc., San Jose, CA. His research interests have spanned the field of semiconductor surface chemistry: ultrahigh vacuum chemical vapor deposition (UHV-CVD) of SiGe films; photochemistry on wide bandgap semiconductor surfaces; TiO<sub>2</sub>

photoanalysis for environmental applications; advanced processing technology for microelectronic materials; and process diagnostics, simulation, and control.

Dr. Lu received a CGP fellowship from the Chinese Education Commission in 1985, and a Graduate Student Prize and the Varian Award, both from the American Vacuum Society in 1990. He is a member of the American Chemical Society, the American Vacuum Society, and the American Association for the Advancement of Science.



**Monalisa Bora** received the B.Tech degree in electrical and electronics engineering from the Indian Institute of Technology, Madras, India, in 1993 and the M.S. degree in electrical and computer engineering from North Carolina State University (NCSU), Raleigh, in 1996.

She is currently an Engineer with Actel Corporation, Sunnyvale, CA. Her research interests are in the design and integration of semiconductor devices and processes; modeling, simulation, and analysis of logistics and process; and manufacturing systems

optimization using simulation.

Ms. Bora received a National Science Foundation fellowship from the Engineering Research Center for Advanced Electronic Materials Processing, NCSU, in 1994.

**Laura L. Tedder** received the Ph.D. degree in chemistry from the University of California, San Diego

She did postdoctoral work at the NSF Engineering Research Center for Advanced Electronic Materials Processing, North Carolina State University, Raleigh. She is currently the Associate Director of Education at the Optoelectronic Computing Systems Center, University of Colorado, Boulder.



**Gary W. Rubloff** (M'87-SM'93) received the B.A. degree in physics from Dartmouth College, Hanover, NH, in 1966, and the Ph.D. degree in physics from the University of Chicago, Chicago, IL, in 1971.

He is currently Director of the Institute for Systems Research and Professor, Department of Materials and Nuclear Engineering, University of Maryland, College Park. Following a postdoctoral appointment in physics at Brown University, Providence, RI, he was a Research Staff Member and held various management positions in physical sciences, silicon technology, and manufacturing research at the IBM Thomas J. Watson Research Center, Yorktown Heights, NY, from 1973 to 1993. From 1993 to 1996, he was Associate Director of the NSF Engineering Research Center for Advanced Electronic Materials Processing and Professor of Electrical and Computer Engineering, North Carolina State University, Raleigh. His research interests have spanned solid state and surface physics; semiconductor interfaces, materials, and process technology; ultraclean, integrated processing and advanced equipment; and advanced diagnostic techniques. His current research efforts are aimed at real-time process sensing, dynamic simulation for design optimization, process control, environmentally-conscious manufacturing, and manufacturing education and training. He has published more than 100 papers and holds 15 U.S. patents.

Dr. Rubloff is a founding chairman of the AVS Manufacturing Science and Technology Group, a Fellow of APS and AVS, and is active in semiconductor roadmapping activities.